

Supporting Information

A Catalyst-Free Synthesis of B, N Co-Doped Graphene Nanostructures with Tunable Dimensions as Highly Efficient Metal free Dual Electrocatalysts

Hassina Tabassum, Ruqiang Zou, Asif Mahmood, Zibin Liang, Shaojun Guo**

Beijing Key Laboratory for Theory and Technology of Advanced Battery Materials,
Department of Materials Science and Engineering, College of Engineering, Peking University,
Beijing 100871, China

E-mail: rzhou@pku.edu.cn; guosj@pku.edu.cn

Figures

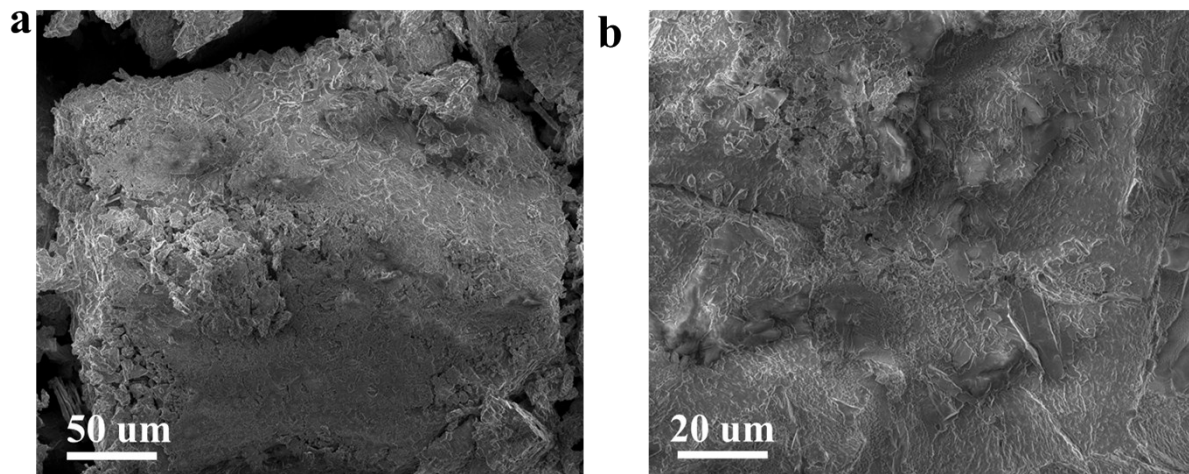


Figure S1. (a, b) SEM images of dried BCN precursor powder at different magnification.

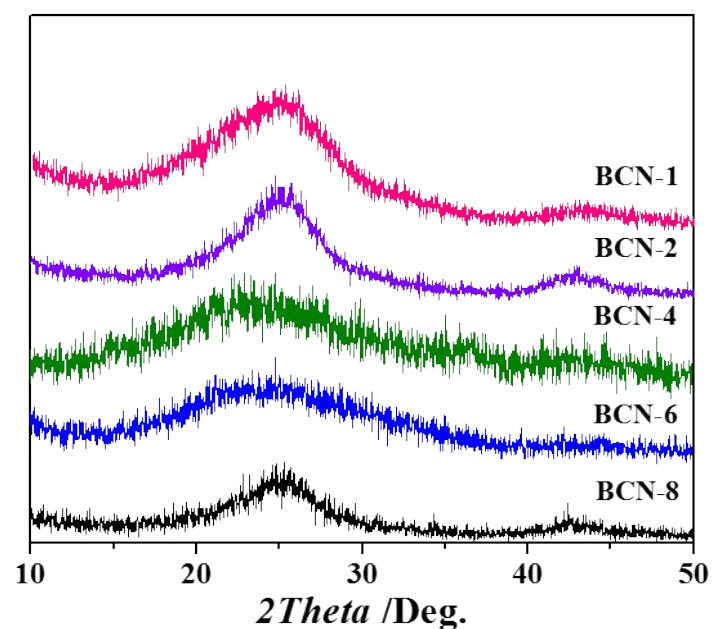


Figure S2. XRD pattern of BCN allotrope.

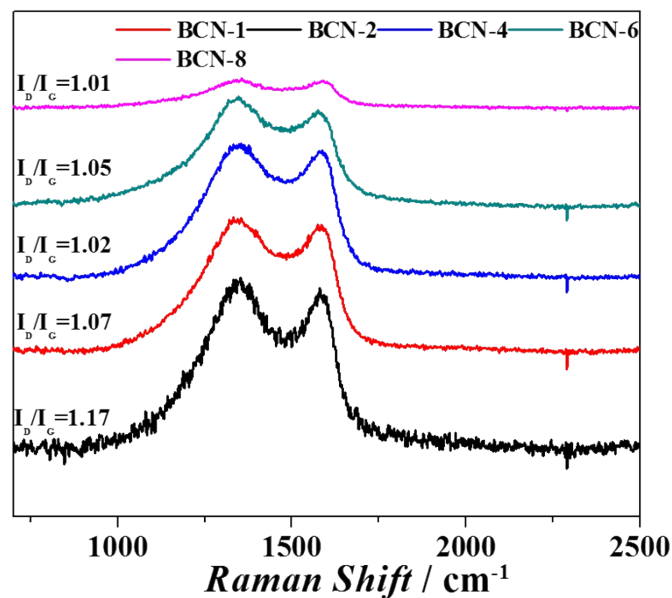


Figure S3. Raman spectra of BCN allotrope.

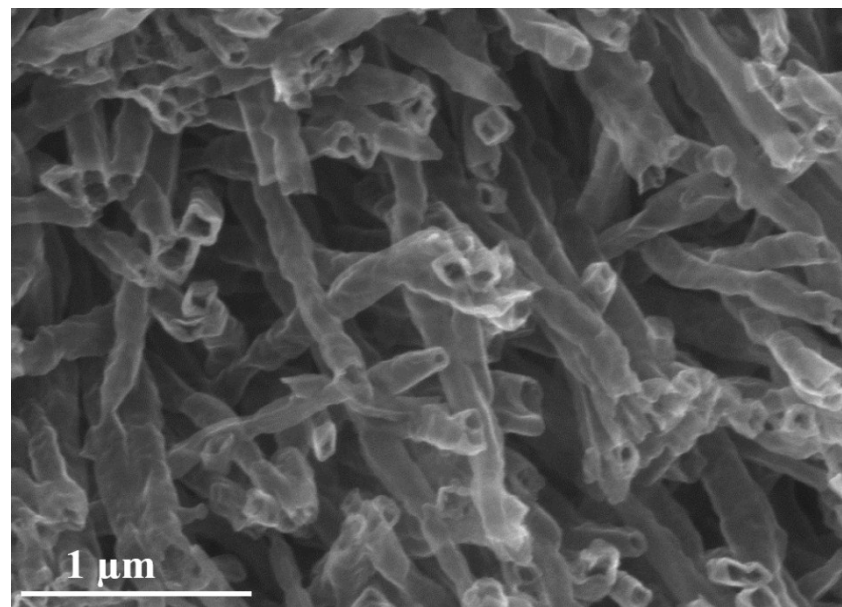


Figure S4. FESEM image of BCN-2 nanotubes at low magnification.

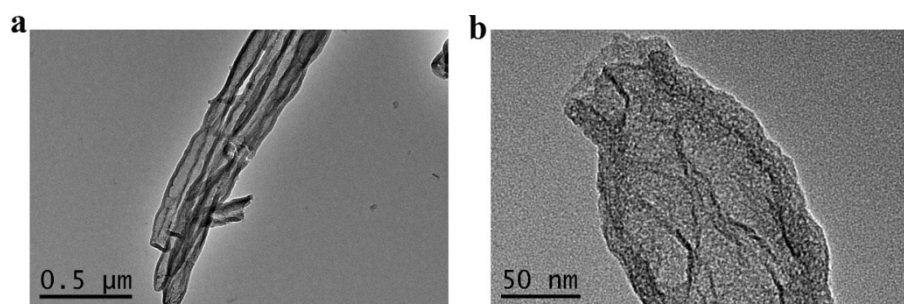


Figure S5. TEM image of BCN-2 nanotubes at different magnifications.

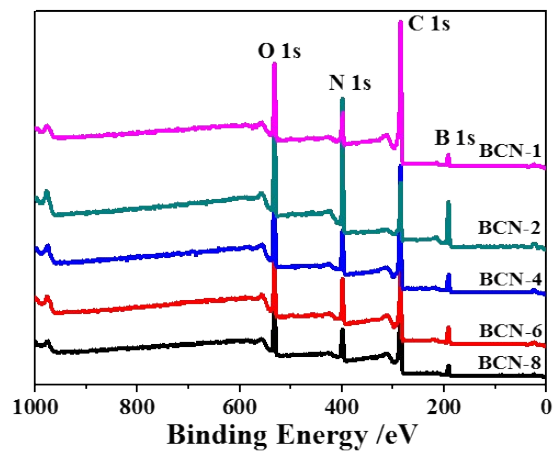


Figure S6. XPS survey of BCN allotropes.

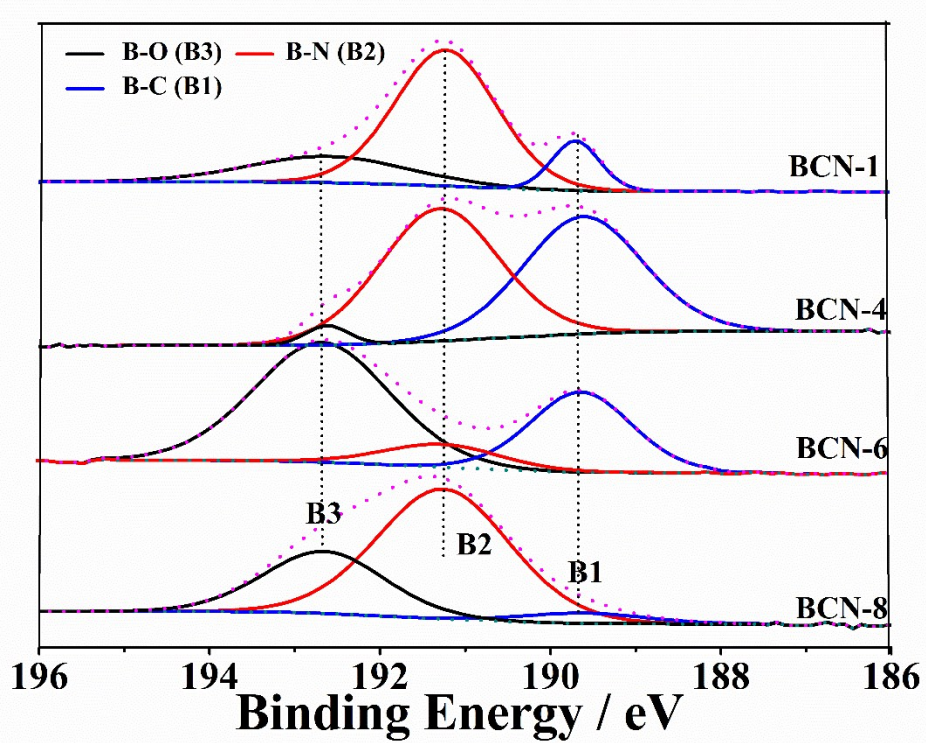


Figure S7. XPS analysis of B-moieties in BCN allotropes.

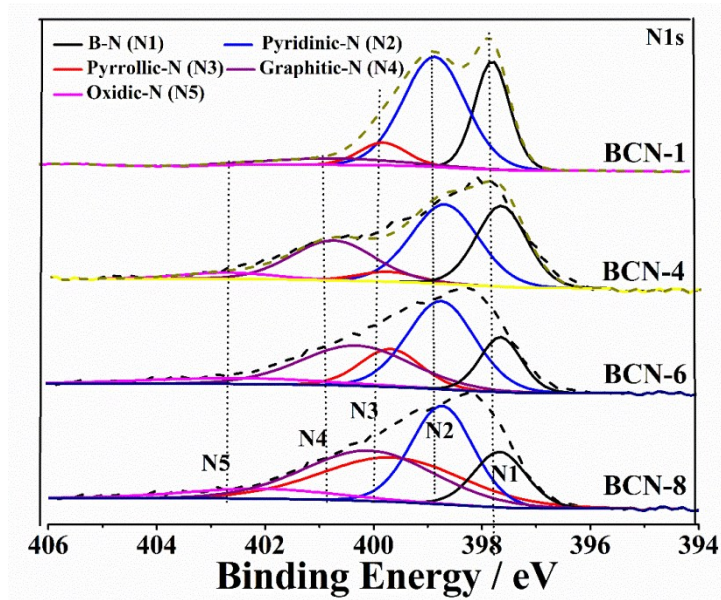


Figure S8. XPS analysis of N-moieties in BCN allotropes.

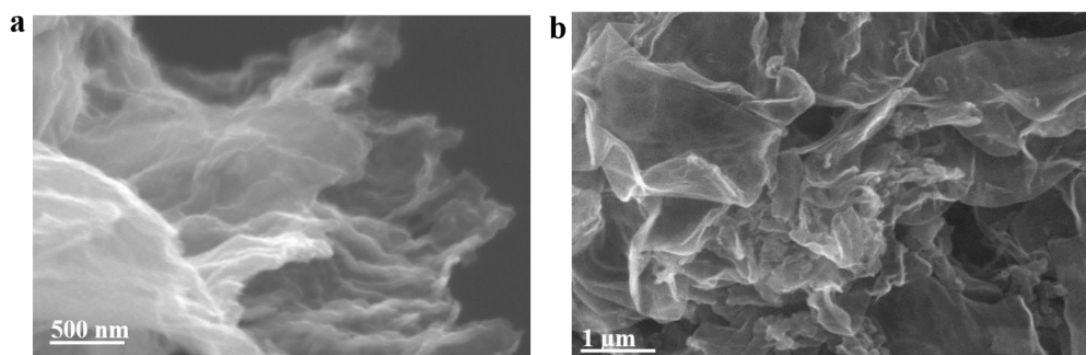


Figure S9. (a, b) FESEM image of BCN-8 nanosheets.

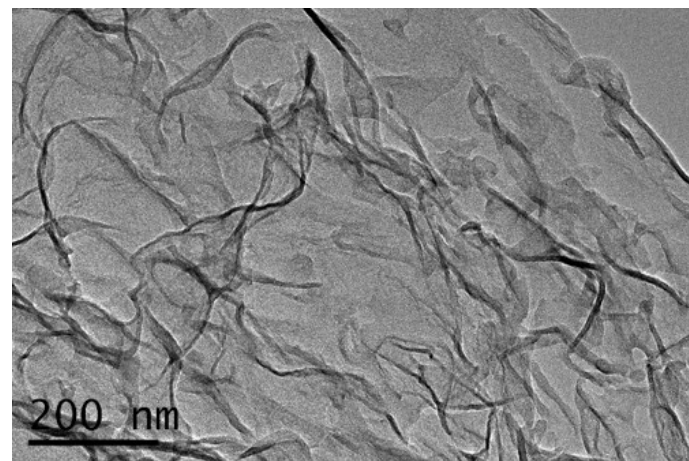


Figure S10. TEM image of BCN-8 nanosheets.

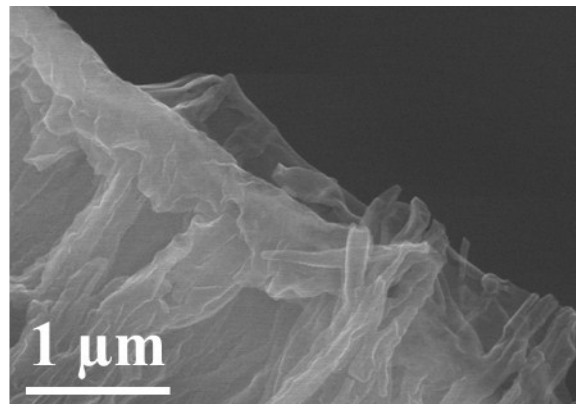


Figure S11. FESEM image of BCN-6 nanosheets.

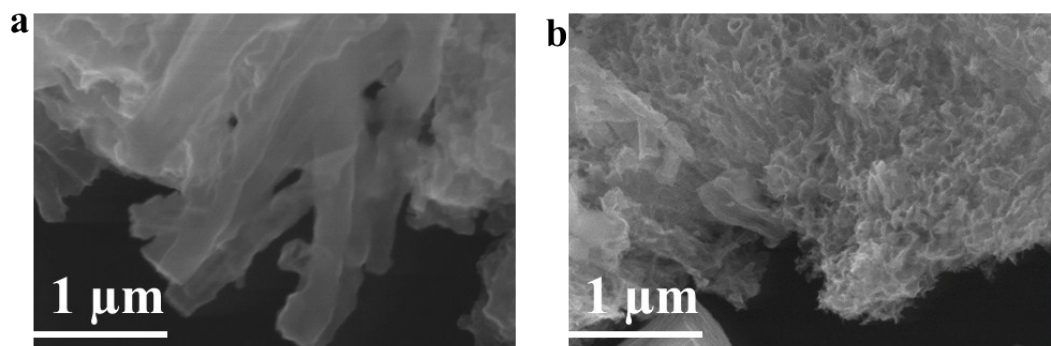


Figure S12. FESEM image of BCN-4 (partially nanotubes).

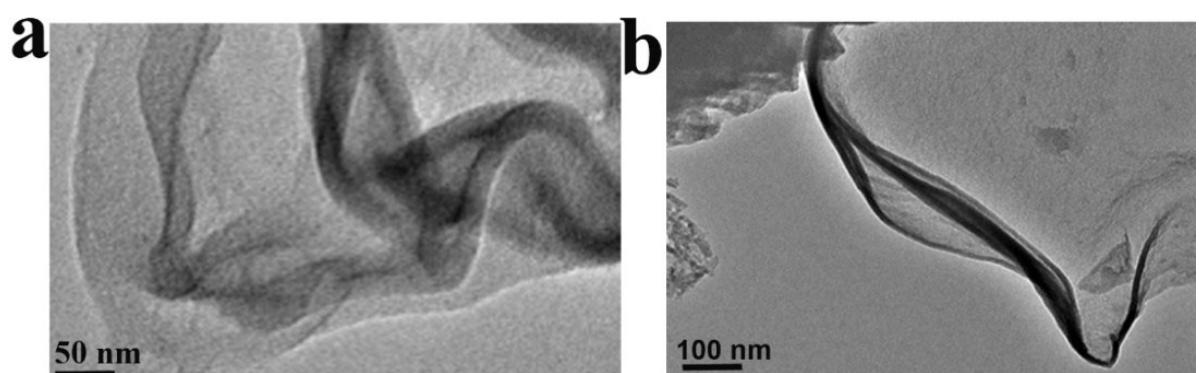


Figure S13. FESEM image of BCN-6 nanotubes at different magnifications.

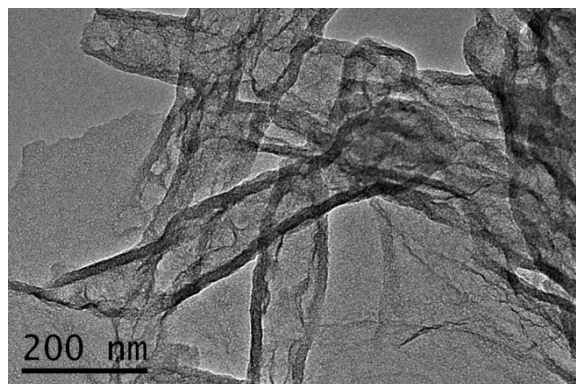


Figure S14. TEM image of BCN-4 (partial nanotubes).

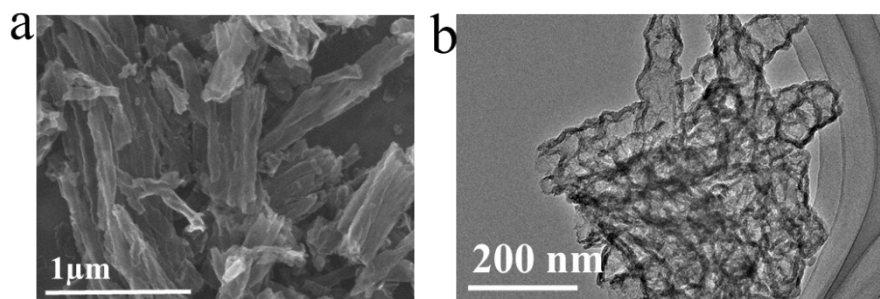


Figure S15. (a) FESEM and (b) TEM image of BCN-1 nanotubes.

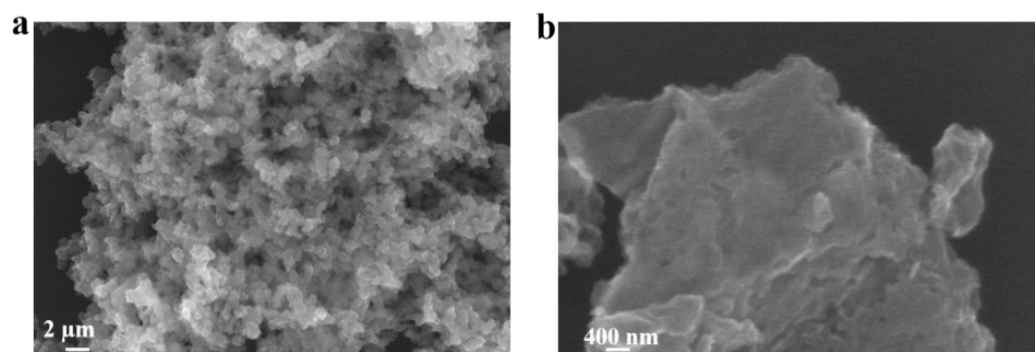


Figure S16. FE-SEM image of (a) BC-2 and (b) CN-2.

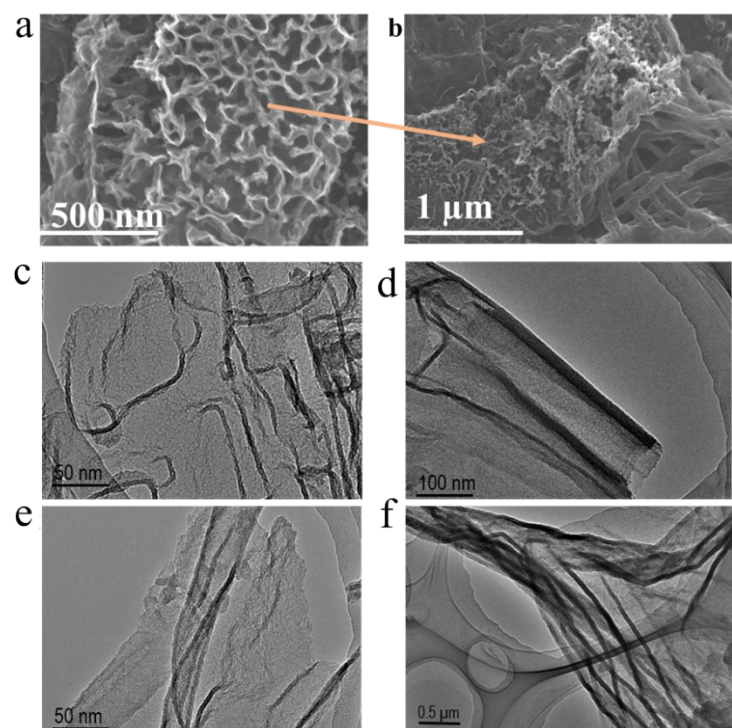


Figure S17. (a, b) FESEM image and (c, d) TEM images of BCN-2-800 °C at different magnifications.

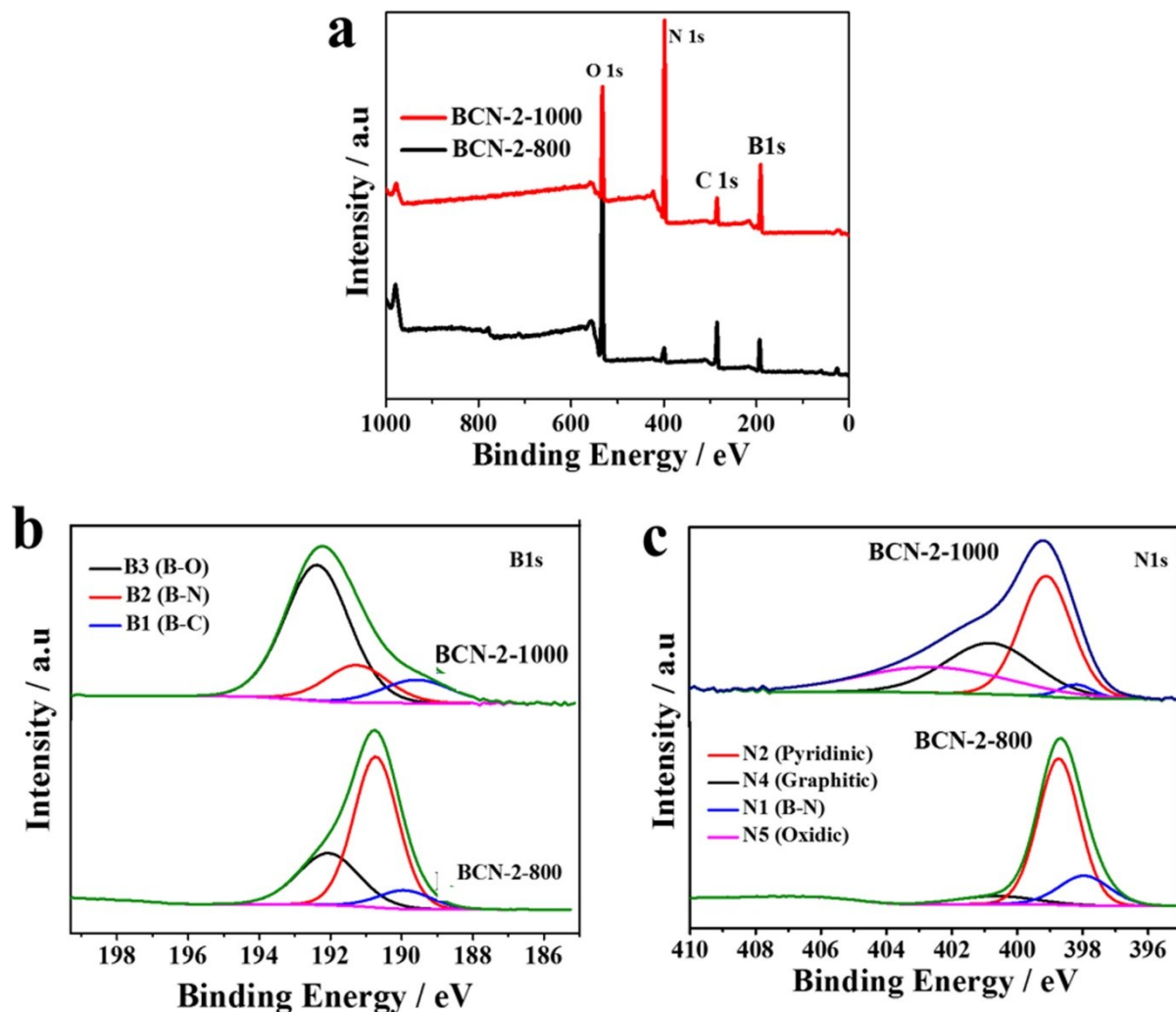


Figure S18. (a) XPS survey, (2) B1s and (c) N1s spectra of BCN-2-800 and BCN-2-1000.

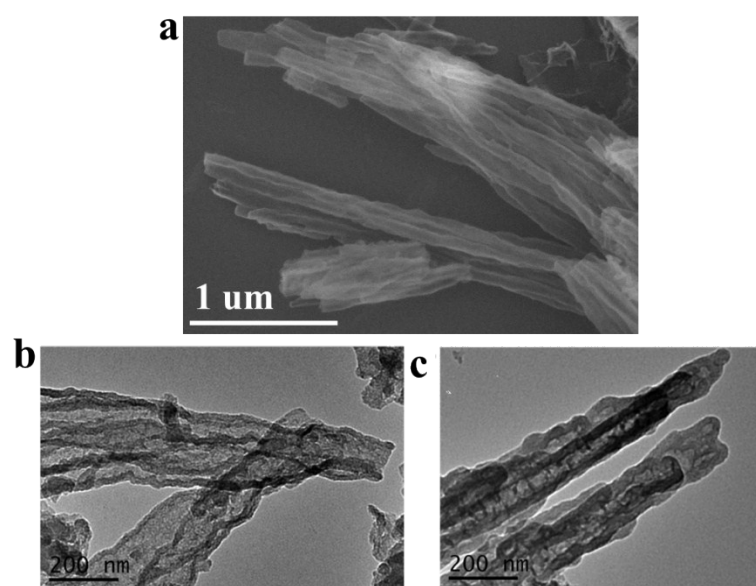


Figure S19. (a) FESEM and (b, c) TEM image of BCN-2-1000 nanotubes.

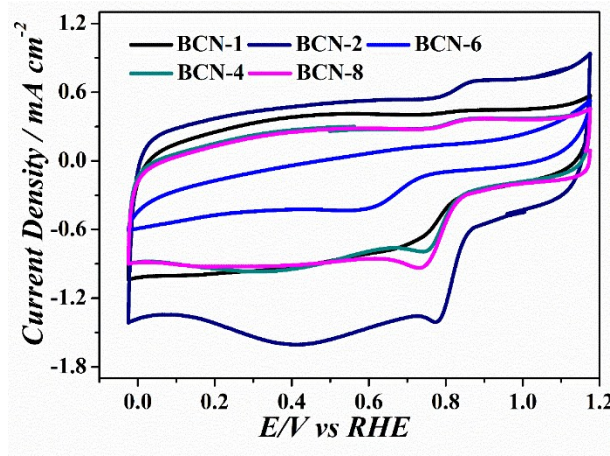


Figure S20. CVs of BCN nanostructures in O₂-saturated 0.1 M KOH solution.

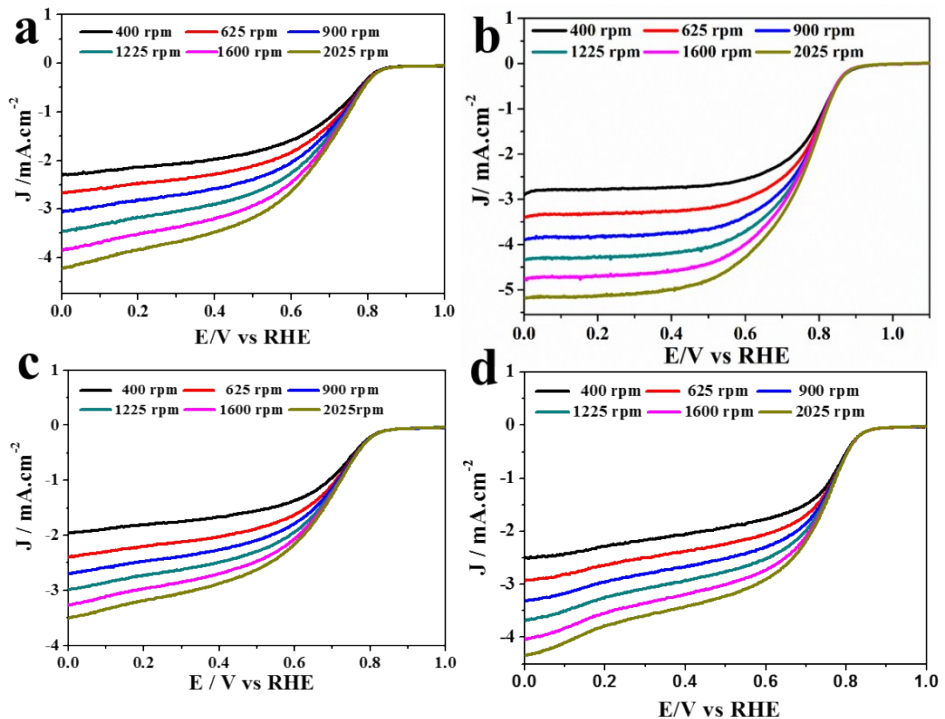


Figure S21. LSV curves of (a) BCN-1, (b) BCN-4, (c) BCN-6 and (BCN-8) at different rotating rates.

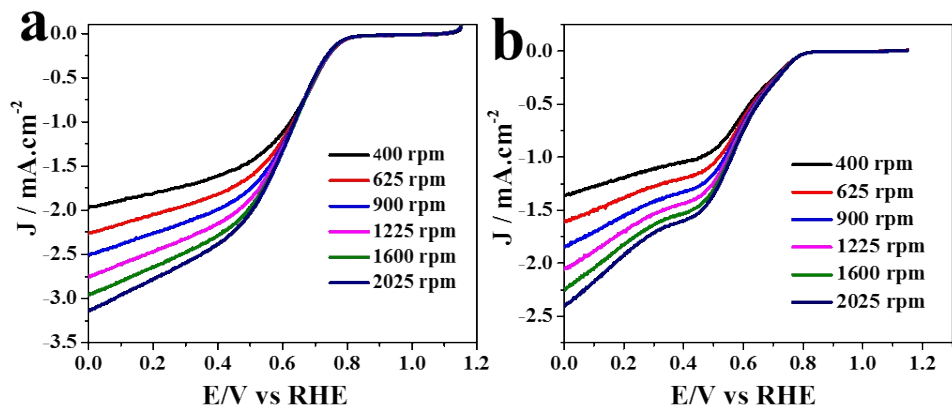


Figure S22. ORR LSV curves of (a) BC-2 and (b) CN-2 products.

The number (n) of electron transfer on the catalysts was determined by using Koutechy-Levich (K-L) equation (see below).

$$\frac{1}{J} = \frac{1}{J_L} + \frac{1}{J_K} = \frac{1}{\frac{1}{B\omega^2}} + \frac{1}{J_K} \quad (S1)$$

$$B = 0.62nFC_o(D_o)^{\frac{2}{3}}v^{\frac{-1}{6}} \quad (S2)$$

$$J_K = nFkC_o \quad (S3)$$

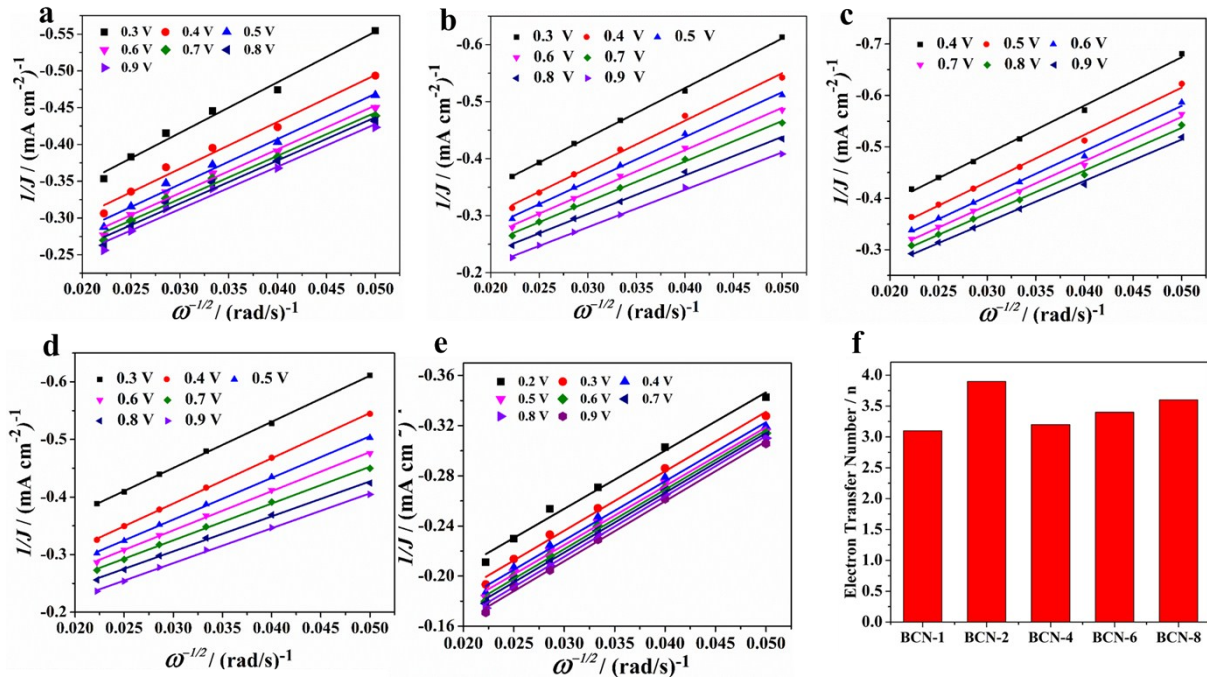


Figure S23. (a-e) K-L plots and (f) the corresponding electron transfer number of (a) BCN-1, (b) BCN-4, (c) BCN-6, (d) BCN-8 and (e) BCN-2 at different voltages.

The given below equation was used for finding the Tafel slope for HER.

$$\eta = a + b \log \left(\frac{i}{i_o} \right) \quad (S4)$$

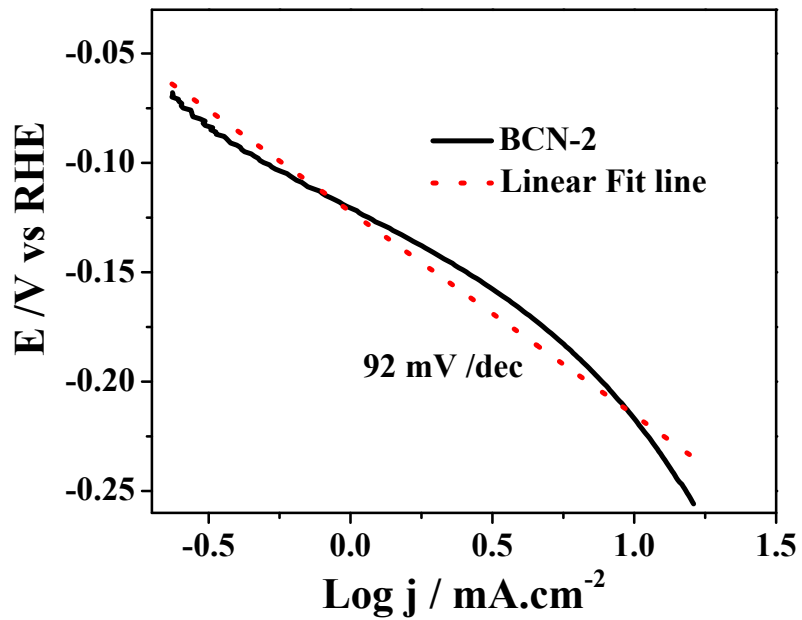


Figure S24. Tafel slope of BCN-2 nanotubes for HER activity.

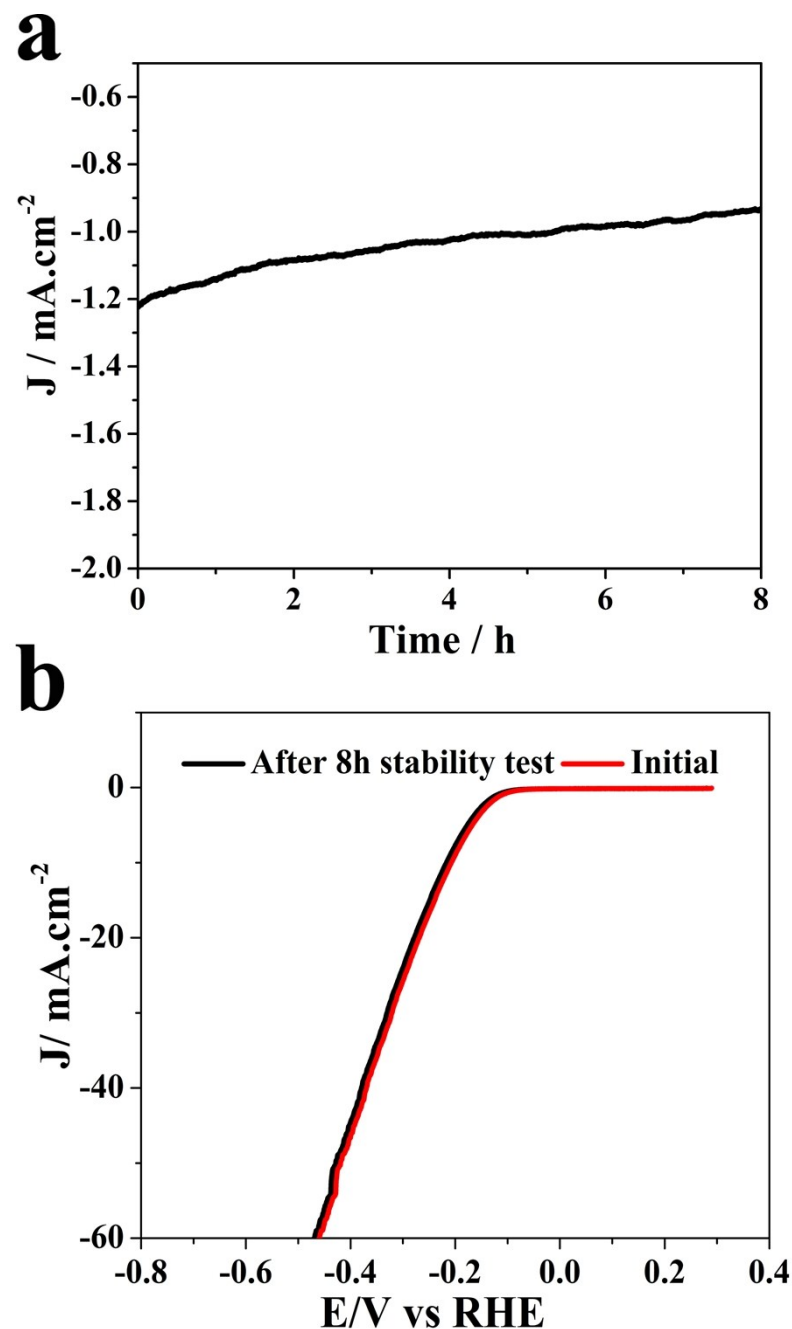


Figure S25. Chronoamperometric measurement of BCN-2 nanotubes for HER stability. HER polarization curves before and after 8h stability test.

Table S1. Elemental compositions of BCN nanostructures determined by ICP for boron content and elemental analyzer for carbon and nitrogen.

Sample Name	Nitrogen %	Boron %	Carbon%	Oxygen%
BCN-1	14.94	13.18	68.52	3.36
BCN-2	15.06	16.66	66.20	1.08
BCN-4	8.38	14.09	73.5	4.03
BCN-6	7.96	12.19	76.10	3.04
BCN-8	8.1	11.96	77.04	3.9

Table S2. Surface elemental quantification of BCN allotropes determined by XPS.

Sample Name	B/ %	N/%	C/%	O/%
BCN-1	12.55	10.98	71.9	4.57
BCN-2	7.3	11.35	80.18	1.17
BCN-4	9.91	8.10	73.09	8.90
BCN-6	10.23	9.02	78.25	2.5
BCN-8	10.36	10.35	71.19	8.10
BCN-2-800	15.53	18.77	50.7	15.0
BCN-2-1000	10.88	10.36	61.11	17.65

Table S3. XPS B1s deconvoluted peaks area% for the distribution of B-moieties.

Atomic Bonds of B /%	Binding Energy / eV	BCN-1	BCN-2	BCN-4	BCN-6	BCN-8	BCN-2-800	BCN-2-1000
B-C	189.6	28.40	73.2	56.76	46.26	4.92	9.05	12.65
B-N	191.2	59.9	15.3	32.2	19.56	61.1	61.82	18.29
B-O	192.6	11.7	11.5	11.04	34.44	33.98	29.13	69.06

Table S4. XPS N1s deconvoluted peaks area% for the distribution of N-moieties.

Atomic Bonds of N / %	Binding Energy / eV	BCN-1	BCN-2	BCN-4	BCN-6	BCN-8	BCN-2-800	BCN-2-1000
N-graphitic	400.6	3.92	39.93	27.31	17.06	10.92	7.48	2.98
B-N	397.6	32.47	2.93	33.01	8.60	4.7	18.49	1.89
N-pyridinic	398.7	30.8	43.68	18.15	26.8	48.01	74.03	41.64
N-pyrrolic	399.6	26.20	11.70	17.02	37.52	31.18	-	41.64
N-oxidic	402.4	6.61	1.76	4.51	10.02	5.19	2.51	25.56

Table S5. BET surface area and pore volume of BCN allotropes.

Sample Name	BET surface area (m^2g^{-1})	Pore volume
BCN-1	746	0.58
BCN-2	890	0.88
BCN-4	652	0.57
BCN-6	721	0.19
BCN-8	547	0.38

Table S6. Comparisons of ORR performance with BCN-2 and state-of-the-art carbon nanomaterials.

Doped Carbon architecture	Onset Potential / mV vs RHE	Half wave Potentials /V vs RHE	Electron transfer Number (n)	References
BCN-2	0.92	0.82	3.92	This work
BCN nanosheets	0.65	0.73	3.98	[1]
B doped CNT	0.66	0.74	3.9	[2]
Graphitic- C ₃ N ₄ @carbon	0.457	0.74	4	[3]
h-BCN nanosheets	0.9	0.76	4	[4]
B,N doped Nanotube	0.89	0.73	4	[5]
B graphene	0.857	0.657	2.5	[6]
B, N co-doped graphene sphere	0.8	0.69	3.3	[7]
B, N graphene quantum dots	0.95	0.55	3.93	[8]
Pt/C	0.99	0.84	4	Commercial

Table S7. Comparisons of HER performance with BCN-2 and state-of-the-art carbon nanomaterials.

Doped Carbon	Overpotential (η) (mV) vs RHE at 10 mA.cm ⁻²	Tafel slope value	References
N/S co-doped graphene	300	81	[9]
B/N co-doped carbon nanosheets	330	100	[10]
B doped graphene	490	99	[11]
N, P co-doped carbon network	298	89	[12]
C ₃ N ₄ @NG nanosheets	240	51	[13]
N doped hexagonal carbon	270	89	[14]
BCN-2	216	92	This Work

References

- [1] Y. Zheng, Y. Jiao, L. Ge, M. Jaroniec, S. Z. Qiao, *Angew. Chem., Int. Ed.* **2013**, *52*, 3110-3116.
- [2] Y. A. Kim, S. Aoki, K. Fujisawa, Y. I. Ko, K. S. Yang, C. M. Yang, Y. C. Jung, T. Hayashi, M. Endo, M. Terrones, M. S. Dresselhaus, *J. Phys. Chem. C* **2014**, *118*, 4454-4459.
- [3] Y. Zheng, Y. Jiao, J. Chen, J. Liu, J. Liang, A. Du, W. M. Zhang, Z. H. Zhu, S. C. Smith, M. Jaroniec, G. Q. Lu, S. Z. Qiao, *J. Am. Chem. Soc.* **2011**, *133*, 20116-20119.
- [4] J. Jin, F. Pan, L. Jiang, X. Fu, A. Liang, Z. Wei, J. Zhang, G. Sun, *ACS Nano* **2014**, *8*, 3313-3321.
- [5] Y. Zhao, L. Yang, S. Chen, X. Wang, Y. Ma, Q. Wu, Y. Jiang, W. Qian, Z. Hu, *J. Am. Chem. Soc.* **2013**, *135*, 1201-1204.
- [6] L. J. Yang, S. J. Jiang, Y. Zhao, L. Zhu, S. Chen, X. Z. Wang, Q. Wu, J. Ma, Y. W. Ma, Z. Hu, *Angew. Chem., Int. Ed.* **2011**, *50*, 7132-7135.
- [7] Z. Jiang, X. Zhao, X. Tian, L. Luo, J. Fang, H. Gao, Z.-J. Jiang, *ACS Appl. Mater. Interfaces* **2015**, *7*, 19398-19407.
- [8] H. Fei, R. Ye, G. Ye, Y. Gong, Z. Peng, X. Fan, E. L. G. Samuel, P. M. Ajayan, J. M. Tour, *ACS Nano* **2014**, *8*, 10837-10843.
- [9] Y. Ito, W. T. Cong, T. Fujita, Z. Tang, M. W. Chen, *Angew. Chem., Int. Ed.* **2015**, *54*, 2131-2136.
- [10] M. Chhetri, S. Maitra, H. Chakraborty, U. V. Waghmare, C. N. R. Rao, *Energy Environ. Sci.* **2016**, *9*, 95-101.
- [11] B. R. Sathe, X. Zou, T. Asefa, *Catal. Sci. Technol.* **2014**, *4*, 2023-2030.
- [12] J. T. Zhang, L. T. Qu, G. Q. Shi, J. Y. Liu, J. F. Chen, L. M. Dai, *Angew. Chem., Int. Ed.* **2016**, *55*, 2230-2234.
- [13] Y. Zheng, Y. Jiao, Y. H. Zhu, L. H. Li, Y. Han, Y. Chen, A. J. Du, M. Jaroniec, S. Z. Qiao, *Nat. Commun.* **2014**, *5*.
- [14] Y. Liu, H. Yu, X. Quan, S. Chen, H. Zhao, Y. Zhang, *Sci. Rep.* **2014**, *4*, 6843.